EXPERIMENTAL VERIFICATION OF A MOISTURE AND HEAT TRANSFER MODEL IN THE HYGROSCOPIC REGIME

D.M. Burch
Member ASHRAE

R.R. Zarr

A.H. Fanney, Ph.D.
Member ASHRAE

ABSTRACT

The National Institute of Standards and Technology (NIST) has developed a personal computer model, called MOIST, for predicting the transient moisture and heat transfer within building envelopes. This paper summarizes selected results from a comprehensive laboratory experiment conducted to verify the accuracy of the computer model in the hygroscopic regime.

This paper discusses three different multilayer wall specimens installed in a calibrated hot box. The exterior surfaces of the wall specimens were first exposed to both steady and time-dependent winter conditions, while their interior surfaces were maintained at 21°C (70°F) and 50% relative humidity. These boundary conditions caused moisture from the interior environment to permeate into the wall specimens and accumulate in their exterior construction materials. Subsequently, the exterior air temperature was elevated to 32°C (90°F), and the exterior construction materials lost moisture to the interior environment. The moisture content within the exterior construction materials and the heat transfer rate at the inside surface of the wall specimens were measured and compared to computer predictions. The moisture and heat transfer properties for the construction materials comprising the wall specimens were independently measured and used as input to the computer model.

The agreement between predicted and measured moisture contents was within 1.1% moisture content. Predicted and measured heat transfer rates also were in close agreement. Accumulated moisture was observed to have little effect on heat transfer because moisture did not accumulate above the hygroscopic limit (i.e., the so-called fiber saturation point) and capillary water did not exist within the pore space of the materials. The insulation remained relatively dry, and the boundary conditions did not give rise to a latent heat effect (i.e., water was not induced to evaporate from one part of the construction and condense in another part).

INTRODUCTION

This paper summarizes selected results from a comprehensive laboratory experiment (Zarr et al. 1995) to verify the accuracy in the hygroscopic regime[1] of a computer model, called MOIST (Version 2.1), that predicts heat and moisture transfer in building envelopes. This research project is part of an ongoing international research activity to experimentally verify mathematical models that predict heat, air, and moisture movement within building envelopes. Modeling exercises currently are being conducted by Annex 24 of the International Energy Agency to address all aspects of moisture movement.

As part of the experiment, three different multilayer wall specimens[2] were built and assembled collectively in a calibrated hot box. The exterior construction layers consisted of hygroscopic materials that permitted moisture accumulation and facilitated the measurement of moisture content. The first wall specimen was composed of gypsum board, fiberglass insulation, and exterior wood siding. The second wall specimen was the same, except that it contained a cavity air space instead of fiberglass insulation, thereby permitting the effect of cavity insulation to be investigated. The third wall specimen was the same as the first, except that it included fiberboard sheathing, thereby permitting the effect of sheathing to be investigated. The boundary conditions were selected to prevent moisture from accumulating above fiber saturation levels within the materials.

A calibrated hot box (Zarr et al. 1987) provided controlled temperature and relative humidity conditions at the interior and exterior surfaces of the wall specimens. The wall specimens were first preconditioned to provide the desired initial moisture contents in their construction materials. During the experiment, the exterior surfaces

[1]Here the term *hygroscopic regime* means that the materials absorbed moisture by sorption at relative humidities below saturation (100%) and capillary water did not exist within the pore space of the materials.
[2]Twelve wall specimens were included in the laboratory experiment. This paper reports the results of three wall specimens.

Douglas M. Burch, Robert R. Zarr, and **A. Hunter Fanney** are with the National Institute of Standards and Technology, Gaithersburg, MD.

of wall specimens were exposed to a sequence of winter conditions that caused moisture to permeate into the wall specimens and accumulate within the exterior construction materials. The interior surfaces of the wall specimens were maintained at 21°C (70°F) and 50% relative humidity. Subsequently, the ambient temperature at the exterior surfaces of the wall specimens was elevated to 32°C (90°F), causing the exterior construction materials to lose moisture to the interior environment. The moisture content of the exterior construction materials and the inside surface heat flux of the wall specimens were measured and compared to corresponding computer predicted values.

OVERVIEW OF MOIST

Several models have been developed to predict moisture and heat transfer within building envelopes. The features and capabilities of these models are compared by Hens and Janssens (1993). One such public domain model, developed at the National Institute of Standards and Technology (NIST), is MOIST (Burch and Thomas 1992).

MOIST predicts the one-dimensional heat and moisture transfer within building envelopes and predicts the construction material moisture content vs. the time of year. It includes moisture transfer in the diffusion (hygroscopic) regime through the capillary flow regime, and includes important couplings between heat and moisture transfer.[3] The model includes one-dimensional algorithms to model a constant flow rate of indoor or outdoor air to an internal air cavity. The model predicts the incident solar radiation onto surfaces having various orientations and tilt. Other features include graphics that display the average moisture content of the construction layers vs. time and a catalog of heat and moisture transfer properties for common building materials. The mathematical algorithms used in the model are described in Burch and Thomas (1992).

The computer model permits users to easily define a wall or cathedral ceiling and predict the moisture content of the various construction materials as a function of time. The type and placement of building materials can be varied. By comparing predicted results with and without a vapor retarder, the model can be used to determine whether a vapor retarder is needed and, if so, where it should be placed. It also can be used to evaluate the effect of various paints and wall coverings on moisture accumulation. In addition, the model allows users to electronically "move" a wall or ceiling to different U.S. and Canadian cities to investigate the effect of climate on moisture accumulation. Hourly weather data for six U.S. cities are provided with the model. Weather data for 40 other U.S. and five Canadian cities are available from the American Society of Heating, Refrigerating and Air-Conditioning Engineers (ASHRAE) (Crow 1981).

In working with a model, it is always important to acknowledge its limitations. One of the most significant limitations of MOIST is that it is one dimensional. This means that it does not include the effect of thermal bridges and framing members and the multidimensional effects associated with air movement due to wind and stack effects. The model does not include the effect of freezing liquid water on the moisture properties of materials, nor does it include moisture absorption from driving rain. In spite of these limitations, the authors believe that predictions with computer models, such as MOIST, can provide useful information to building practitioners on the moisture performance of various building envelope constructions. It is worth mentioning that more complex models accommodating these limitations are not currently in the public domain.

[3]The *diffusion regime* includes moisture transfer by vapor diffusion through the open pore space and bound water transfer by hygroscopic action. The *capillary regime* includes Darcy (liquid) flow through the pore space of the materials.

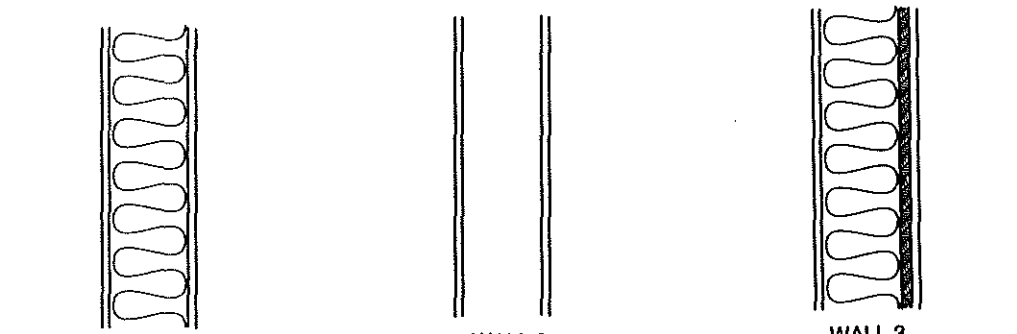

Figure 1 *Wall specimen construction details.*

DESCRIPTION OF THE EXPERIMENT

Wall Specimens

The construction details of the three wall specimens analyzed in this paper are given in Figure 1. Each wall specimen had overall dimensions of 1.0 m by 1.1 m (3.3 ft by 3.6 ft) and was installed in the support frame of the calibrated hot box as shown in Figure 2a. Each wall specimen contained a center metering section circumscribed by a thin, 0.03-mm (0.001-in.) plastic sleeve that minimized lateral moisture flow and provided one-dimensional moisture transfer within the metering section. A special series of moisture content measurements (Zarr et al. 1995) was conducted on the inside surface of the sugar pine of wall specimen 1 and revealed that the lateral distribution in moisture content was within ±1.6% moisture content. A finite-difference analysis was conducted and revealed that the heat transfer within the metering area also was one dimensional.

Calibrated Hot Box

The support frame and the assembled wall specimens were installed between the metering chamber and the climatic chamber of the calibrated hot box, as shown in Figure 2b. The metering chamber provided a downward airstream at the interior surface of the wall specimens that was maintained at 21.2°C ± 0.1°C (70.2°F ± 0.2°F) and 50% ± 3% relative humidity during the entire experiment. The climatic chamber generated an upward airstream at the exterior surface of the wall specimens. The climatic chamber boundary conditions are given below.

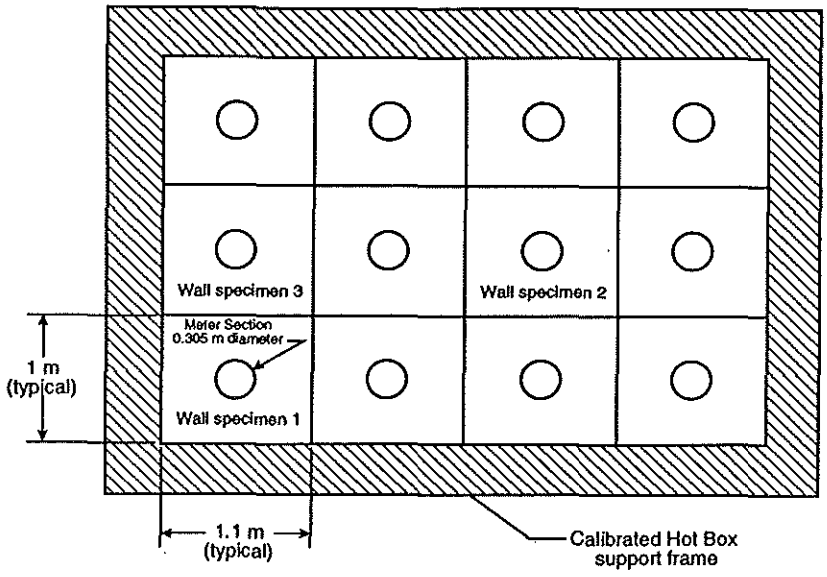

a. Wall specimen location within support frame of calibrated hot box.

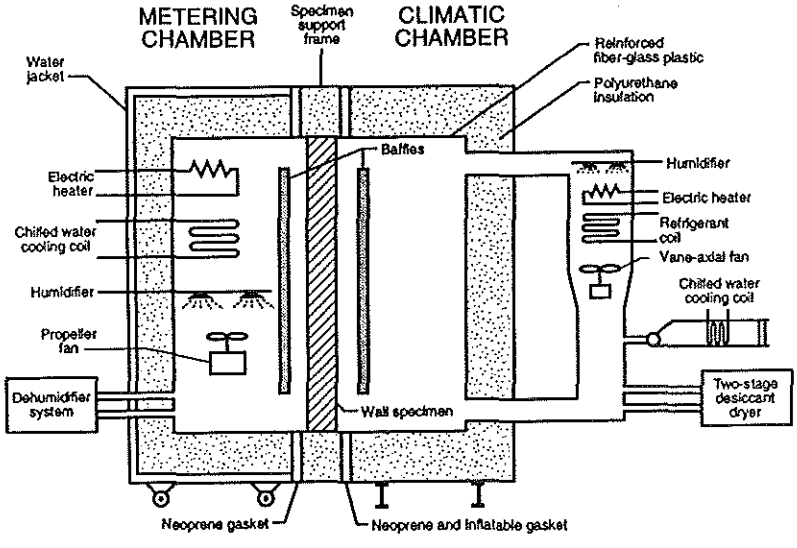

b. Schematic of NIST Calibrated Hot Box.

Figure 2 *Description of experiment.*

Climatic Chamber Boundary Conditions

After the wall specimens were preconditioned for 42 days, the climatic chamber ambient temperature was programmed to generate the sequence of temperature conditions given in Table 1. The ambient temperature and relative humidity maintained inside the climatic chamber during the experiment, and preconditioning periods are plotted in Figure 3. Note that the ambient relative humidity maintained in the climatic chamber ranged between 3% and 11% during the experiment period. Such a low relative humidity was necessary to minimize frost accumulation on the chamber's refrigeration coil. The authors acknowledge that such a low relative humidity is atypical of prevailing outdoor winter relative humidities.

TABLE 1 **Climatic Chamber Conditions**

Condition	Days
Winter - Steady	1
Winter - Diurnal Sinewave[a]	6
Winter - Steady	34
Winter - Diurnal Sinewave[a]	7
Summer - Steady	14

[a]The diurnal sinewave had a mean value of 7.2°C (45°F), an amplitude of 17°C (31°F), and a period of 24 hours.

The four winter conditions caused moisture from the interior environment to permeate into the wall specimens and accumulate in their exterior construction materials as a function of time. The purpose of the first and second series of diur-

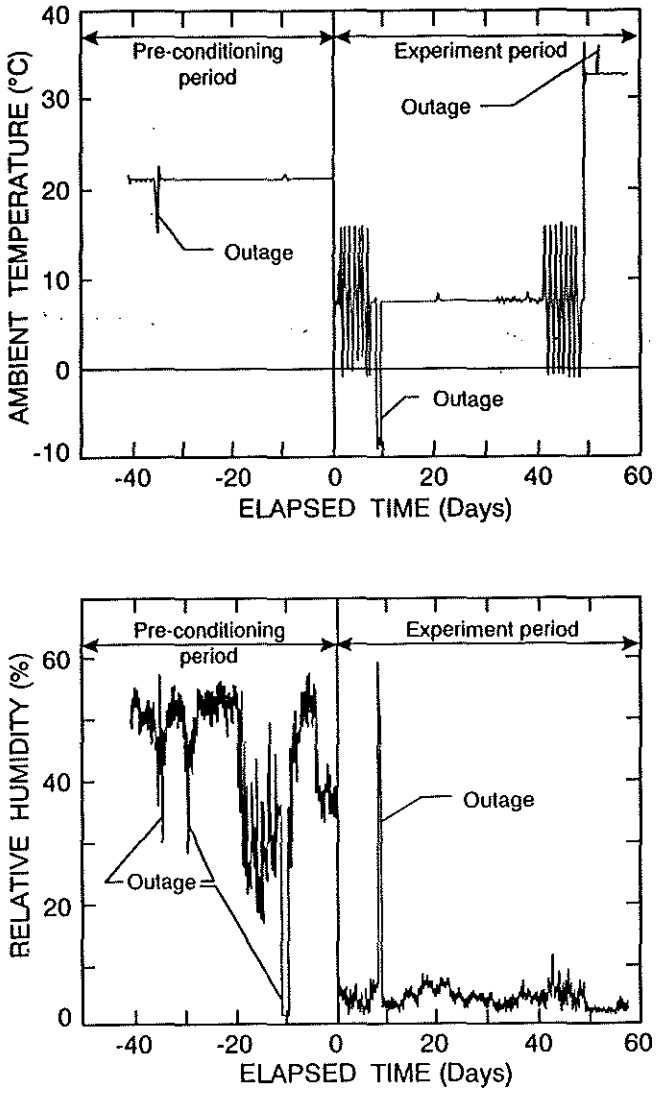

Figure 3 *Climatic chamber boundary conditions.*

nal sinewaves was to provide a comparison of the diurnal heat transfer rate during periods when the wall specimens were comparatively dry and moist. During the final summer period, the exterior ambient temperature was elevated to 32°C (90°F), causing the exterior construction materials to lose moisture to the interior environment.

INSTRUMENTATION

The metering section of each wall specimen was instrumented as shown in Figure 4a. The ambient temperature was measured at a distance of approximately 50 mm (2 in.) from the inside and outside surfaces of the wall specimens. The heat flux was measured at the interior surface of the gypsum board. The moisture content and surface temperature were measured at the interior surface of the sheathing (if present) and both the interior and exterior surfaces of the sugar pine.

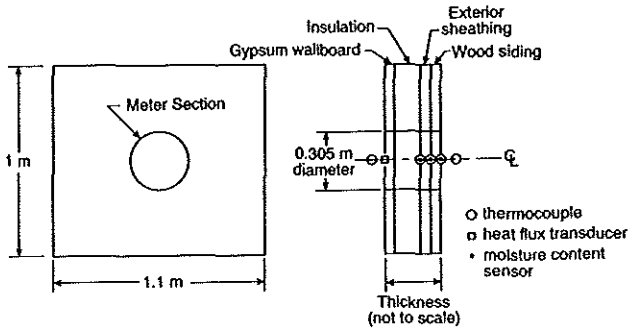

a. Wall specimen sensor location.

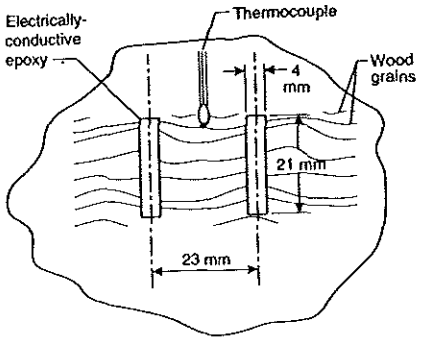

b. Construction of moisture content sensor.

Figure 4 *Description of instrumentation.*

The ambient relative humidity was measured at the center of the airstreams on opposite sides of the wall specimens using calibrated capacitance-type relative humidity transducers. Calibrated thermocouple wire was used for the temperature measurements. Details relating to the moisture content and heat flux measurements are given below.

Moisture Content

The moisture content of the wood-based materials was measured using the electrical-resistance method (Duff 1968). This method is based on the principle that, below fiber saturation, there exists a unique relationship between moisture content and electrical resistance for different species of wood and other building materials. For this experiment, a commercial moisture meter with a display resolution of 0.1% moisture content was used. The two-pin metal electrodes supplied with the meter were replaced with a pair of parallel electrically conductive epoxy strips applied to the surface of the wood-based materials (see Figure 4b). The epoxy was applied to the surface of the wood-based materials in strips normal to the wood grain, as illustrated in Figure 4b. Using a template, the mixture was applied to the surface of the material as two strips, each approximately 4 mm (0.16 in.) wide with a centerline-to-centerline spacing of 23 mm (0.91 in.). Before curing, bare-wire leads were

placed in the mixture (one lead per strip). The mixture was allowed to cure at room temperature for a minimum of 24 hours.

After the experiment, the moisture content sensors were individually calibrated. This calibration was accomplished by removing the sensors from their corresponding wall specimen with a 100-mm by 100-mm (4-in. by 4-in.) section of the substrate material. The sensors were then placed inside a precision temperature and humidity chamber that conditioned the substrate materials to various moisture contents at ambient temperatures of 4.4°C (39.9°F) and 32.2°C (90.0°F). For each sensor, the relationship between the metered moisture content and the actual moisture content was established at the two ambient temperature conditions. During the calibrated-hot-box experiment, the effect of temperature on the moisture content measurements was included by linear interpolation.

Heat Flux

The heat flux at the center of the metered section of each of the wall specimens was measured using a small heat flux transducer attached to the gypsum board using a silicone-rubber adhesive. The transducers were 23 mm (0.91 in.) in diameter and 3.2 mm (0.125 in.) thick. These heat flux transducers generated a DC voltage signal directly proportional to the magnitude of the heat flux passing through the transducer. The heat flux transducers were calibrated by exposing them to known heat fluxes in the NIST guarded hot plate and establishing a relationship between millivolt output and heat flux.

MATERIAL PROPERTY MEASUREMENTS

The material properties for the wall specimens were independently measured and input to the model to minimize uncertainties associated with material variability. The property measurements included sorption isotherm measurements, permeability measurements, and thermal conductivity measurements and are summarized below. Further information on the property measurements is given in Zarr et al. (1995).

Sorption Isotherm Measurements

The sorption isotherms were determined by placing eight small specimens of each hygroscopic material in vessels above saturated salt-in-water solutions. Each saturated salt-in-water solution provided a fixed relative humidity (Greenspan 1977). The vessels were maintained at a temperature of 24°C ± 0.2°C (75°F ± 0.4°F) until the specimens reached steady-state equilibrium. The equilibrium moisture content was plotted vs. relative humidity to give the sorption isotherm. Separate sorption isotherm data were obtained for specimens initially dry (adsorption isotherm) and for specimens initially saturated (desorption isotherm). A detailed description of this measurement method is given in Richards et al. (1992).

The mean of the absorption and desorption isotherm measurements was fit to an equation of the following form:

$$\gamma = \frac{B_1\phi}{(1 + B_2\phi)\,(1 - B_3\phi)} \quad (1)$$

where

γ = moisture content, and
ϕ = relative humidity

The coefficients B_1, B_2, and B_3 were determined by regression analysis and are summarized in Table 2.

TABLE 2 **Sorption Isotherm Regression Coefficients**

Materials	B_1	B_2	B_3
Fiberboard sheathing	1.14	50.6	0.923
Glass-fiber insulation	0.00170	$1 \cdot 10^{-8}$	0.963
Gypsum wallboard	0.00336	$1 \cdot 10^{-8}$	0.901
Sugar pine	0.192	2.05	0.765

The uncertainty in the sorption isotherm measurements was within ±1.5% moisture content.

Permeability Measurements

The water-vapor permeability of the hygroscopic materials was measured using permeability cups placed in controlled environments. Five circular specimens, 140 mm (5.5 in.) in diameter, of each material were sealed at the top of open-mouth glass dishes. The dishes were subsequently placed inside sealed-glass vessels maintained at a constant temperature. Saturated salt-in-water solutions were used inside the glass dish and surrounding glass vessels to generate a relative humidity difference of approximately 10% across each specimen. By using different salt solutions, the mean relative humidity across the specimen was varied over the humidity range of 11% to 97%. Permeability was plotted vs. the mean relative humidity across the specimen. Separate measurements conducted at 7°C (45°F) and 24°C (75°F) revealed that temperature has a small effect on permeability over this temperature range. A detailed description of the permeability measurement method is given in Burch et al. (1992). The materials used in the wall experiment experienced temperatures somewhat outside the range of the permeability measurements.

Water vapor permeability data were plotted vs. the mean relative humidity across the specimen and fit to an equation of the form:

$$\mu = \exp(C_1 + C_2\phi + C_3\phi^2). \quad (2)$$

Here the permeability (μ) is expressed in $kg/s \cdot m^2 \cdot Pa$. The coefficients C_1, C_2, and C_3 were determined by regression analysis and are summarized in Table 3.

The permeance of fiberglass insulation was assumed to be equal to measurements of the permeability of a

TABLE 3 Vapor Permeability Regression Coefficients

Materials	C_1	C_2	C_3
Fiberboard sheathing	-24.054	- .1004	0.0
Fiberglass insulation	-22.425	0.0	0.0
Gypsum wallboard	-23.475	0.0	0.0
Sugar pine	-28.677	-0.9198	4.576

The uncertainty in measuring the permeance of the materials was less than 5% when measuring materials having a permeance less than 5.7×10^{-11} kg/s·m²·Pa (10 perm). However, the uncertainty increased rapidly as the specimen permeance rose above 5.7×10^{-11} kg/s·m²·Pa (10 perm).

stagnant air layer. This assumption is reasonable because the glass fibers of the insulation occupy a small fraction of its volume. In this situation, bound-water diffusion along the glass fibers is small compared with molecular diffusion through the predominantly open pore space. The Lewis relationship between heat and mass transfer (Threlkeld 1970) was used to calculate a water vapor permeance of $13{,}300 \times 10^{-12}$ kg/s·m²·Pa for the cavity airspace of wall specimen 2.

Heat Transfer Properties

The thermal conductivities of the materials were measured in accordance with ASTM Test Method C 177 (ASTM 1993) using the NIST guarded hot plate. Each measurement was carried out at approximately the same mean temperature that the material experienced during the steady-state winter condition of the experiment. The thermal conductivity of the fiberglass insulation was determined at the same thickness and density as in the wall cavities. The densities of the materials were measured, and their specific heats were taken from ASHRAE (1993). The heat transfer properties for the materials are summarized in Table 4.

TABLE 4 Heat Transfer Properties of the Materials

Materials		Density (kg/m³)	Specific Heat (J/kg·K)	Thermal Conductivity (W/m·K)
Fiberboard Sheathing		380.4	1300	0.0539
Gypsum Wallboard		628.6	1090	0.159
Sugar Pine		373.8	1630	0.0865
Glass-fiber Insulation	Wall 1	9.1	805	0.0445
	Wall 3	8.8	805	0.0450

The density of the glass-fiber insulation was determined by extracting an in situ core sample of the insulation in-line with the heat flux transducer. The thermal conductivity subsequently was calculated from a conductivity vs. density correlation. The uncertainty in measuring the thermal conductivity was less than 1%.

The specimens were preconditioned at 21°C ± 2°C (70°F ± 1°F) and 40% to 60% relative humidity for about two months prior to the guarded hot plate measurements.

COMPARISON OF MEASURED AND PREDICTED MOISTURE CONTENTS

In this section, the measured moisture contents of the exterior construction materials are compared to computer-predicted values. The measured boundary conditions and material properties were used as input to the model. In the finite-difference analysis, two nodes were used in the gypsum board, seven in the sheathing material (if present), and seven in the sugar pine.[4] A one-hour time step was used. The insulation was treated as a nonstorage layer (i.e., the storage of heat and moisture was neglected). The predicted surface moisture contents were based on a 3.2 mm (0.125 in.) thick layer of the material at the respective surfaces.

Wall Specimen 1 (Fiberglass Insulation)

The moisture content at the inside surface of the sugar pine for wall specimen 1 (base case) is given in Figure 5a. The measured and predicted values are indicated by the solid and dashed lines, respectively. At time zero, the exterior ambient temperature decreased from 21°C (70°F) to 7.2°C (45°F) (see Figure 3) and water vapor from the interior environment diffused into the wall construction and accumulated in the sugar pine. The surface moisture content increased to approximately 25% moisture content (moisture content) after 48 days. Subsequently, the ambient temperature at the exterior surface of the wall was increased to 32°C (90°F). Consequently, the moisture content at the inside wood surface decreased rapidly. The sinusoidal moisture content variations were caused by the diurnal sinewave variations in the climatic chamber temperature shown in Figure 3. The amplitude of the variations in moisture content are about 2% moisture content.

The average difference between the measured and predicted moisture content was expressed as a root-mean-square difference, or

$$\delta_{RMS} = \sqrt{\frac{\sum_{n=1}^{N} (\Delta_n)^2}{N}} \quad (3)$$

where Δ_n is the instantaneous difference between the measured and predicted values, and N is the number of values in the data set. The δ_{RMS} for wall specimen 1 was 1.1% moisture content, indicating good agreement between the predicted and measured values.

It was not possible to compare the measured and predicted moisture contents at the exterior surface of the sugar pine because the moisture content decreased below the minimum detectable moisture content (i.e., 6%) of the moisture meter within a few hours after the start of the experiment. This sudden drop in moisture content occurred because the exterior wood surface was exposed to ambient air having a 3% to 11% relative humidity.

[4]This number of nodes were sufficient to achieve convergence of the mathematical solution. That is, computer predictions with twice as many nodes in each material gave virtually identical results.

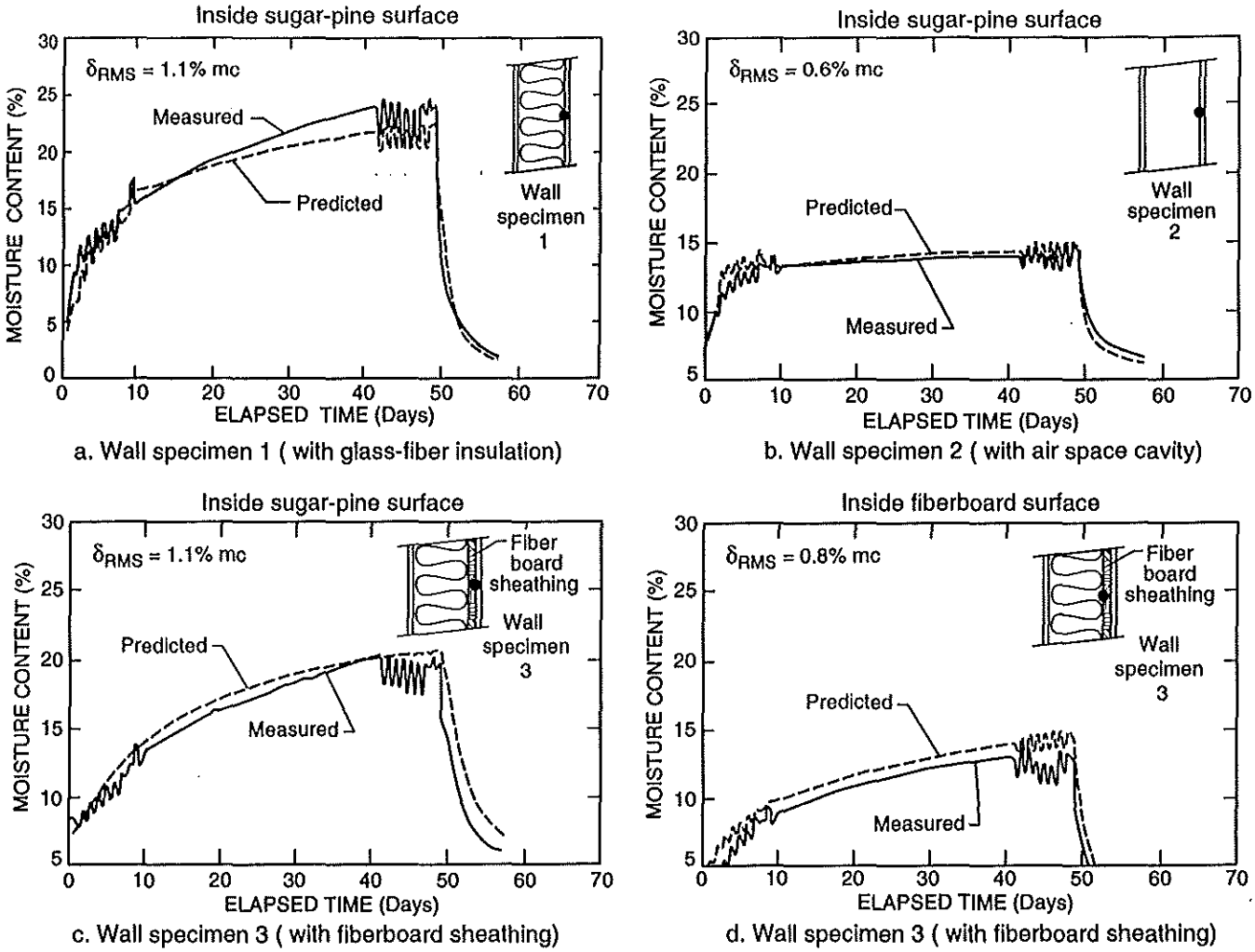

Figure 5 *Comparison of measured and predicted moisture content for wall specimens.*

It is worth noting that the moisture content at the inside sugar pine surface rose almost to fiber saturation (27% moisture content) when the exterior wall surface was exposed to a "mild" winter condition. These results indicate that, when a wall is airtight and has no interior vapor retarder, vapor diffusion can cause high moisture content in exterior construction materials.

Wall Specimen 2 (Airspace)

The results for wall specimen 2 are given in Figure 5b. This wall is identical to wall specimen 1, except that no thermal insulation was installed in the cavity, forming an airspace. The δ_{RMS} is 0.6% moisture content, indicating good agreement between the measured and predicted moisture contents.

Comparing Figures 5a and 5b, the measured peak moisture content rose to 14% with an air cavity and 25% with insulation in the cavity. The placement of thermal insulation in the wall cavity increased the peak moisture content at the sugar pine by approximately 11%. An explanation is that the thermal insulation decreases the heat transfer and reduces the sugar pine temperature, providing a larger temperature difference for driving moisture transfer.

Wall Specimen 3 (Fiberboard Sheathing)

A comparison between measured and predicted moisture contents for wall specimen 3 is given in Figures 5c and 5d. This wall is identical to wall specimen 1, except that fiberboard sheathing is installed between the insulation and the sugar pine. The δ_{RMS} is 0.81% moisture content at the inside fiberboard surface and 1.1% moisture content at the inside sugar pine surface, indicating good agreement between measured and predicted moisture contents.

Comparing Figures 5a and 5c, it is seen that the addition of the fiberboard sheathing reduces the peak moisture content at the sugar pine by 6%. An explanation is that the fiberboard sheathing provides additional moisture-storage capacity for the wall construction. A portion of the moisture inflow is stored in the fiberboard sheathing instead of the sugar pine.

In summary, the agreement between predicted and measured moisture contents for these three wall specimens was within 1.1%. The authors are unable to explain the source of error giving rise to random and systematic differences between measured and predicted results.

Several simple steady-state calculation methods, such as the dew-point method (ASHRAE 1993) and Glaser's method (1959), can be used to predict the moisture accumulation in walls exposed to boundary conditions that induce condensation. A steady-state dew-point method calculation was performed on wall specimen 1 to determine whether it could accurately predict the moisture accumulation at the inside wood surface for this particular experiment. The results are given in the appendix. The dew-point method was found to be sensitive to assumed values for the vapor diffusion resistance of the wood. That is, the calculation results varied markedly as the vapor diffusion resistance was varied over a reasonable range. Another shortcoming of the dew-point method is that it does not predict the variation in moisture content (or relative humidity) across the wood. In this experiment, the wood layer has a relatively high vapor diffusion resistance. This means that the influx of moisture produced a high moisture content at the inside wood surface, thereby providing a conducive environment for mold and mildew growth.

COMPARISON OF MEASURED AND PREDICTED HEAT TRANSFER RATES

The heat flux measured during the second series of diurnal sinewaves for wall specimen 1 is compared to values predicted by the computer model in Figure 6. In the computer predictions, the fiberglass insulation was modeled as a nonstorage layer (i.e., the storage of heat and moisture was neglected). Similar agreement between predicted and measured heat fluxes was obtained for the other two wall specimens.

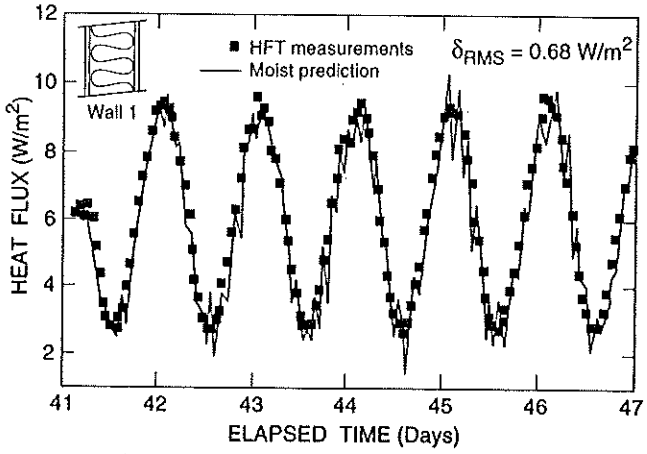

Figure 6 Comparison of measured and predicted heat fluxes for wall specimen 1.

EFFECT OF MOISTURE ON HEAT TRANSFER

To investigate the effect of moisture on heat transfer, the sinusoidal heat flux variations for wall specimen 1 (fiberglass insulation) are compared for the first and second series of sinewaves. The temperature waveforms maintained at the exterior surface of the specimen were virtually identical during the first and second series of sinewaves (Figure 7a). During both periods, the ambient temperature in the metering chamber also was the same. During the first series of sinewaves, the wall specimen was comparatively dry, because insufficient time had elapsed for much moisture to accumulate. During the time between the first and second series of sinewaves, moisture accumulated in the sheathing and siding of the wall specimen. Therefore, the wall specimen contained a considerably larger amount of moisture during the second series of sinewaves compared to that during the first series of sinewaves.

The sinusoidal heat flux variations for the first and second series of sinewaves are compared in Figure 7b. The two sets of heat fluxes are seen to be almost identical. However, the measured heat fluxes tended to have slightly lower peaks during the second series of sinewaves. These results indicate that the accumulation of

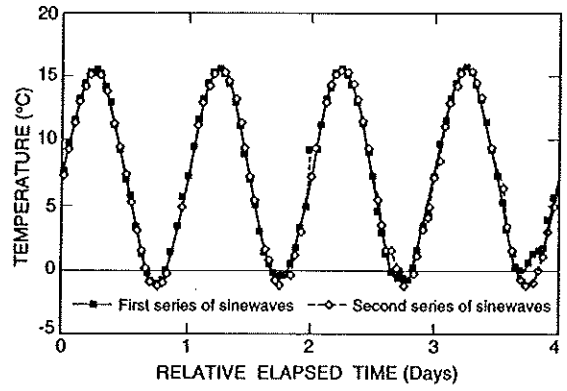

a. Comparison of ambient outdoor temperature (first versus second series of sinewaves)

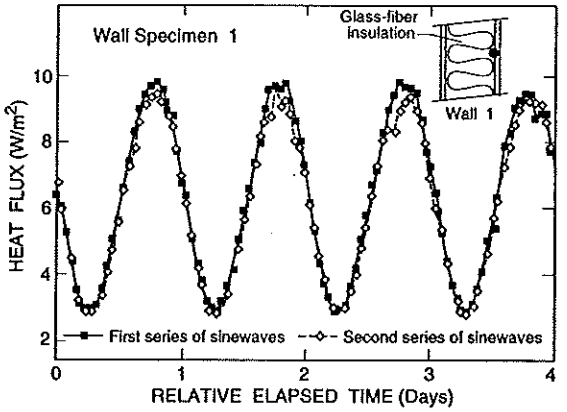

b. Comparison of interior surface heat flux (first versus second series of sinewaves)

Figure 7 Effect of moisture on heat transfer for wall specimen 1.

moisture in the wall specimen had little effect on the heat transfer through the wall specimens.

The authors believe that moisture had a small effect on heat transfer because moisture did not accumulate above the hygroscopic limit of the materials. If moisture had accumulated above the hygroscopic limit and water had existed within the large pore space of the materials, moisture would have had a considerably larger effect on heat transfer because water is considerably more conductive than air. This is particularly true for the insulation, which remained relatively dry during the experiment. In addition, the boundary conditions did not give rise to a latent heat effect (i.e., liquid water was not induced to evaporate from one part of the construction and condense in another part).

SUMMARY AND CONCLUSIONS

A comprehensive experiment was conducted to provide a limited verification of the MOIST computer model in the hygroscopic regime (i.e., the moisture content of materials did not rise above fiber saturation). As part of this experiment, three different multilayer wall specimens were assembled and installed in a calibrated hot box. The wall specimens were instrumented to measure the moisture content of their exterior construction layers and the heat transfer rate at their interior surfaces. The moisture and heat transfer properties for the construction materials were independently measured.

During the experiment, the exterior surfaces of the wall specimens were first exposed to steady and time-dependent winter conditions, while their interior surfaces were maintained at 21°C (70°F) and 50% relative humidity. The winter conditions caused moisture to accumulate within the wall specimens. Subsequently, their exterior surfaces were exposed to an elevated temperature of 32°C (90°F), causing the moisture content within the wall specimens to decrease.

The moisture content of the exterior construction materials and the heat transfer rate at the inside surface of the wall specimens were compared to predictions by the computer model. The agreement between predicted and measured moisture contents was within 1.1% moisture content. The agreement between the predicted and measured heat transfer rates also was good. Accumulated moisture was observed to have little effect on heat transfer because moisture did not accumulate above the hygroscopic limit, therefore, water did not exist within the pore space of the materials, and the insulation remained relatively dry during the experiment. In addition, the boundary conditions did not give rise to a latent heat effect (i.e., water did not evaporate from one part of the construction and condense in another part).

REFERENCES

ASHRAE. 1993. *1993 ASHRAE Handbook—Fundamentals*, chap. 22, Table 4. Atlanta, Ga.: American Society of Heating, Refrigerating and Air-Conditioning Engineers, Inc.

ASTM. 1993. Thermal insulation; environmental acoustics. *Annual Book of ASTM Standards*, vol. 04.06. Philadelphia, Pa.: American Society for Testing and Materials.

Burch, D.M., and W.C. Thomas. 1992. An analysis of moisture accumulation in a wood-frame wall subjected to winter climate. *Proceedings of Thermal Performance of the Exterior Envelopes of Buildings V, ASHRAE/DOE/BTECC Conference, Dec. 7-10, Clearwater Beach, Fla.*

Burch, D.M., W.C. Thomas, and A.H. Fanney. 1992. Water vapor permeability measurements of common building materials. *ASHRAE Transactions* 98(2).

Crow, L.W. 1981. Development of hourly data for weather year for energy calculations (WYEC). *ASHRAE Journal* 23(10): 37-41.

Duff, J.E. 1968. Moisture distribution in wood-frame walls in winter. *Forest Products Journal* 18(1).

Glaser, H. 1959. Graphisches Verfahren zur Untersuchung von Diffusionsvorgänge (Graphical procedures for investigating diffusion). *Kältetechnik* 10: 345-349.

Greenspan, L. 1977. Humidity fixed points of binary saturated aqueous solutions. *Journal of Research, National Bureau of Standards* 81A(1): 89-96.

Hens, H., and A. Janssens. 1993. Enquiry on HAMCat codes. International Energy Agency, Energy Conservation in Buildings and Community Systems Programme. Annex 24. Heat, Air, and Moisture Transfer through New and Retrofitted Insulated Envelope Parts.

Richards, R.F., D.M. Burch, and W.C. Thomas. 1992. Water vapor sorption measurements of common building materials. *ASHRAE Transactions* 98(2).

TenWolde, A. 1994. Design tools, chap. 11 in *Moisture Control in Buildings*, H.R. Trechsel, ed., pp. 208-215. Philadelphia, Pa.: American Society for Testing and Materials.

Threlkeld, J.L. 1970. *Thermal Environmental Engineering*, pp. 196-198. New York: Prentice-Hall.

Zarr, R.R., D.M. Burch, T.K. Faison, C.E. Arnold, and M.E. O'Connell. 1987. Calibration of the NBS calibrated hot box. *Journal of Testing and Evaluation* 15(3).

Zarr, R.R., D.M. Burch, and A.H. Fanney. 1995. Heat and moisture transfer in wood-based wall construction: Measured versus predicted. *Building Science Series 173*. Gaithersburg, Md.: National Institute of Standards and Technology.

APPENDIX

DEW-POINT METHOD CALCULATION

This section examines the accuracy of a simplified technique, the dew-point method[5] (ASHRAE 1993), to predict the amount of condensation buildup within

[5]The dew point method is essentially the same as the European method by Glaser (1959), except that the vapor pressures are plotted vs. vapor diffusion resistance instead of distance.

walls. The method is applied to wall specimen 1, and an attempt is made to predict the moisture accumulation at the inside wood surface during the entire winter condition. The results of the dew-point calculation are given in Figure A1.

At each time step during the entire winter condition, the calculation procedures outlined by TenWolde (1994) were applied to obtain the saturation vapor pressure and vapor pressures for flow continuity vs. distance from the interior wall surface. This graphical procedure is illustrated for the steady winter condition in Figure A1a. The vapor pressure for flow continuity rises above the saturation vapor pressure at the inside wood surface, thereby indicating that the wood surface is a plane of condensation.

When the inside wood surface is determined by the above graphical procedure to be a plane of condensation, the net moisture flux (W''), expressed in kg/s·m^2 (grains/h·ft^2) at the inside wood surface, was predicted by the steady-state equation at each hourly time step:

$$W'' = \frac{P_i - P_s}{R_i + R_1 + R_2} - \frac{P_s - P_o}{R_3 + R_o}$$

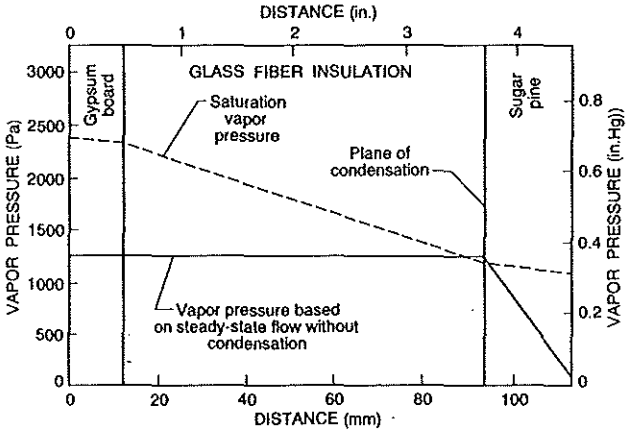

a. Plot of saturation vapor pressure and vapor pressure based on steady-state flow without condensation.

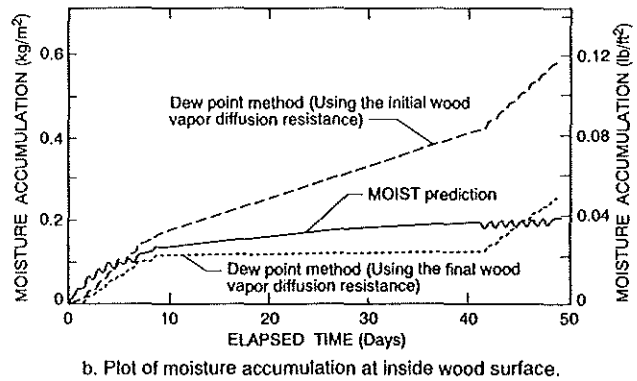

b. Plot of moisture accumulation at inside wood surface.

Figure A1 *Application of dew-point method to wall specimen 1.*

where

P_i = vapor pressure of the inside air, Pa (in. Hg);

P_s = saturation vapor pressure at inside wood surface, Pa (in. Hg);

P_o = vapor pressure of the outside air, Pa (in. Hg);

R_i = inside air film vapor diffusion resistance, s^2·m·Pa/kg (perm^{-1});

R_o = outside air film vapor diffusion resistance, s^2·m·Pa/kg (perm^{-1});

R_1 = gypsum board vapor diffusion resistance, s^2·m·Pa/kg (perm^{-1});

R_2 = fiberglass vapor diffusion resistance, s^2·m·Pa/kg (perm^{-1}); and

R_3 = wood vapor diffusion resistance, s^2·m·Pa/kg (perm^{-1}).

The first term is the influx of moisture from the metering chamber to the plane of condensation, while the second term is the outflux of moisture from the plane of condensation to the climatic chamber. If the inside wood surface is not a plane of condensation (e.g., maximum of diurnal cycle), the net moisture flux was taken to be zero. The moisture accumulation at the plane of condensation was determined by integrating the moisture fluxes over previous time steps.

Two dew-point method calculations were carried out. In the first calculation, the wood vapor diffusion resistance was assumed to be 2.74 × 10^{10} s^2·m·Pa/kg (1.57 perm^{-1}) based on the initial wood moisture content. In the second calculation, the wood vapor diffusion resistance was assumed to be 5.58 × 10^9 s^2·m·Pa/kg (0.321 perm^{-1}) based on the final wood moisture content. The initial and final wood moisture contents were the average moisture content of the wood layer predicted by the MOIST computer model. The moisture accumulations determined by the first and second calculations are compared to corresponding predicted values by the MOIST computer model in Figure A1b. The MOIST values are the moisture accumulation occurring in a 3.2-mm (0.125-in.) inside surface layer of the sugar pine. Because MOIST agreed well with the experimental measurements, it was assumed that it could accurately predict the moisture accumulation at the inside wood surface.

In the first calculation (based on the initial wood vapor diffusion resistance), the dew-point method calculation rises by more than a factor of two above the MOIST prediction. The second dew-point method calculation (using the final wood vapor diffusion resistance) was lower than the MOIST prediction. In this example, the dew-point method calculation is sensitive to assumed values for the wood vapor diffusion resistance.